NEAR FIELD 3D CFD MODELLING OF OVERFLOW PLUMES

L. de Wit[1]

ABSTRACT

Dredging activities can increase turbidity of the ambient waters. One of the most used vessels is a Trailer Suction Hopper Dredger (TSHD). Main causes of increased turbidity of a TSHD are the fine sediments from the overflow plume. Mixing of the overflow plume with cross flowing ambient water is complex and many details are still unknown. A 3D CFD (Computational Fluid Dynamics) model is used to simulate near field mixing of overflow plumes. Initial momentum and density differences of the plume are fully taken into account, state of the art LES (Large Eddy Simulation) technique is used for modelling turbulence. The CFD model has been validated successfully with experimental results. With the CFD model the transition depth, where a overflow plume switches from density driven to mixing by cross flow, is investigated. The obtained transition depths are plotted in a diagram. In this diagram it can easily be seen up to what depth density differences are important for any overflow plume. The results of this study are an extension to the results of Winterwerp (2002).

Keywords: Dredging, TSHD, mixing, transition depth, LES.

INTRODUCTION

This paper describes a 3D CFD (Computational Fluid Dynamics) model to simulate near field mixing of overflow plumes. Overflow plumes are generated by dredging with a Trailing Suction Hopper Dredger (TSHD). TSHDs are widely used for both capital and maintenance dredging. A TSHD sucks up a water-sediment mixture from the seabed and pumps it into its hopper. The water-sediment mixture contains about 20% (volume) solids. Therefore filling of the hopper continues after the hopper is full, by letting the excess water overflow to the ambient water. This excess overflowing water contains a portion of the dredged sediments, which forms a plume. As the settling velocity of fine sediment fractions is lower than the settling velocity of coarser fractions, generally an overflow plume contains more fines than the source material. The increased turbidity levels and/or sedimentation on the bed resulting from overflow can have impact on the aquatic ecosystem. Often an environmental impact assessment and/or intensive monitoring is required for dredging projects. It is therefore needed to understand the behaviour of overflow plumes.

The near field behaviour of overflow plumes is characterised by several interacting, difficult to quantify, processes. There is entrainment of ambient water into the plume and there is interaction with cross flow caused by ambient currents and the trailing speed of a TSHD. This is the pure plume in cross flow behaviour, driven by differences in momentum and density. There are other processes, more specific to dredging, which are also important. A first one is the entrainment of air bubbles in the overflow which can cause a lift effect on the fine particles in the overflow plume. Mixing can be enhanced by the propellers of the TSHD. The flow around the hull of a TSHD, including the boundary layer, may have significant influence. Sediment fractions have a settling velocity which depends on flocculation and interaction with other fractions. Also can there be a large fluctuation in the overflow discharge by raising or lowering the overflow and rolling of the vessel. All these processes make it difficult to predict the behaviour of an overflow plume in near field and thus to predict the proper source amount of fine sediments to the environment. Several measurement campaigns of dredge plumes have been undertaken. Many of them are confidential, but a few have been published, some examples among others are Nakata et al. (1989), Nichols et al. (1990), Whiteside et al. (1995). Unfortunately the results of measurement campaigns are to a large extend site specific and cannot be used in general.

[1] PhD student, Delft University of Technology, Section of Dredging Technology, Mekelweg 2, 2628 CD Delft, Holland, T: +31-(0)15-283583, Email: L.deWit@TUDelft.nl

This paper is written as part of a PhD study at the Dredging Section of the TU Delft which aims to understand and be able to predict the near field behaviour of overflow plumes. A process based 3D CFD model is being developed which, in the end, includes the previous mentioned important processes. State of the art techniques in turbulence and numerics are used to get high quality results. At present, the CFD model can reproduce the pure plume in cross flow behaviour, leaving the other processes to be included later on in the PhD traject. The CFD model is used to find the transition from density-driven behaviour to mixing behaviour. The computational results are validated with experimental data and a comparison with Winterwerp (2002) is made.

First the 3D numerical model is introduced in next section. After that the validation with experimental data is presented, followed by an application to find the transition from density-driven to mixing behaviour. The article ends with the conclusions and recommendations.

3D CFD MODEL

Flow equations

The 3D CFD model is based on the non hydrostatic Navier Stokes equations:

$$\frac{\partial \rho}{\partial t} + \nabla \cdot (\rho \boldsymbol{u}) = 0, \tag{1}$$

$$\frac{\partial \rho \boldsymbol{u}}{\partial t} + \nabla \cdot (\rho \boldsymbol{u}\boldsymbol{u}) = -\nabla P + \nabla \cdot \boldsymbol{\tau} + \rho \boldsymbol{f}, \tag{2}$$

where ρ is the density, $\boldsymbol{u}$ is the velocity vector, t is time, P is the pressure, $\boldsymbol{\tau}$ is a shear stress tensor and $\boldsymbol{f}$ is the acceleration vector due to body forces, like gravity. The first line describes conservation of mass, and the second line conservation of momentum. The density in overflow plumes can be several 100s kg/m^3 higher than the ambient density (Nichols et al. 1990, Nakata et al. 1989). Therefore density variation is fully taken into account, in vertical and both horizontal directions. A mixture approach is used, tracking the concentration of the plume and solving the Navier Stokes equations of the mixture. The plume concentration (volume) C is calculated with a transport equation:

$$\frac{\partial \rho C}{\partial t} + \nabla \cdot (\rho \boldsymbol{u} C) = \nabla \cdot (\rho \Gamma \nabla C), \tag{3}$$

with the diffusion coefficient $\Gamma = \frac{\nu}{Sc}$, a Schmidt number $Sc = 0.7$, and ν is the kinematic viscosity. Using the plume concentration, the mixture density can be obtained by:

$$\rho = \rho_a + (\rho_0 - \rho_a)C, \tag{4}$$

with ρ as the mixture density, ρ_a as the ambient density and ρ_0 as the initial plume density. From the mixture density obtained by Equation 4, the time derivative of the density can be calculated, which is used as input in Equation 1.

The flow equations are solved on a cylindrical coordinate system r, ϕ, z (stream wise, cross, vertical direction). The total model volume has the shape of a piece of pie with a stretched grid following the plume downstream (see Figure 1). In z and ϕ direction an equidistant grid size is used and in r direction a variable grid size. The equations are solved on a staggered grid with the finite volume method using a pressure-correction algorithm. For the resulting pressure Poisson equation a FFT (Fast Fourier Transformation) is used in the equidistant z and ϕ directions and a direct solver for the r direction. This leads to a very fast 3D CFD model, being about 40 times (!) faster than a commercial code like Fluent. Spatial integration is carried out using the second order accurate central scheme, time integration is also second order accurate with the explicit Adams-Bashforth scheme. More details on numerics can be found in Pourquié (1994).

The advection term in the transport equation of the plume concentration is discretised with an accurate TVD (Total Variation Diminishing) scheme. TVD schemes consist of a blend between a second order scheme and a first order

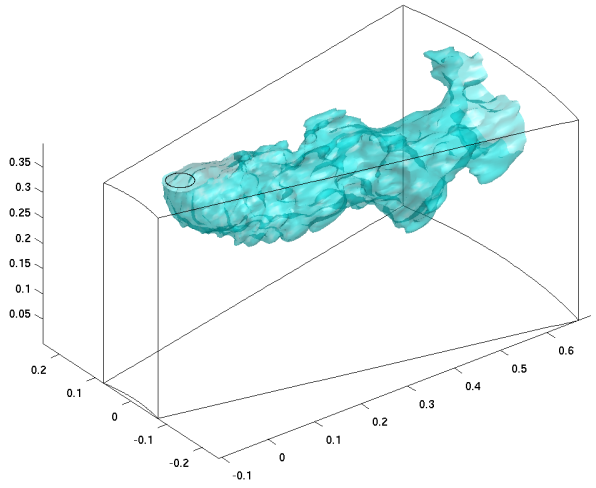

Figure 1: Pie shaped cylindrical grid used to solve overflow plumes.

upwind scheme. A limiter function regulates the blending and with this blending the amount of artificial (numerical) diffusion is controlled. Some limiters in a TVD scheme are known to make gradients artificially sharper (Hirsch 1990). For this study tests were carried out. The Van Leer limiter in the TVD scheme in combination with the 2nd order Adams-Bashforth scheme resulted in the least diffusive results without sharpening gradients.

Turbulence modelling

In Equation 2 a shear stress tensor $\boldsymbol{\tau}$ can be seen. For Newtonian fluids, it can be written as:

$$\boldsymbol{\tau} = \rho_a \nu \left(\nabla \boldsymbol{u} + (\nabla \boldsymbol{u})^T - \frac{2}{3} \nabla \cdot \boldsymbol{u} \right). \tag{5}$$

When all length and time scales up to the smallest Kolmogorov turbulence scales could be solved on the grid, this stress tensor would only consist of a contribution of the molecular viscosity. In real scale problems with high Reynolds numbers however, this is not possible and some kind of filtering is needed. Through this filtering a turbulence contribution to the shear stress tensor is added to the contribution of the molecular viscosity.

Most computational simulations use Reynolds time filtering, leading to RANS (Reynolds Averaged Navier Stokes) equations. In this approach a time filter much larger than the turbulent time scale is used. It makes the flow stationary on turbulent time scale, and leaves it non-stationary on the often much larger time scale of the problem at hand. Using the RANS approach for a plume there are no whirls in the results, but only the smeared out averaged plume. As we are interested in the dynamics of the overflow plume, including the irregularities like whirls, this is not sufficient. In this study we use a LES (Large Eddy Simulation) approach. LES uses a spatial filter. All turbulent fluctuations smaller than the grid size are filtered away and replaced by a sub-grid-scale (sgs) shear stress. In such way all turbulent eddies larger than the grid size are resolved, the price being paid is the need for finer grids than in RANS. Using LES for a plume the most important large whirls are found in simulation results.

In this study the Smagorinsky model is used to calculate the sub-grid-scale viscosity:

$$\nu_{sgs} = (C_s L_f)^2 |\boldsymbol{S}|, \tag{6}$$

where C_s is the Smagorinsky constant (0.1 in this study), L_f is the filter width ($1/3\sqrt{\Delta r^2 + (r\Delta\phi)^2 + \Delta z^2}$), and $\boldsymbol{S}$ is the rate of strain tensor. The total viscosity is found by adding the sub-grid-scale viscosity by the molecular

viscosity:

$$\nu = \nu_{mol} + \nu_{sgs}. \tag{7}$$

Boundary conditions

On the upstream and two lateral boundaries inflow conditions are applied. On outflow a zero pressure is used and a Von Neumann condition for the other parameters ($\frac{\partial}{\partial n} = 0$). See Figure 2 for a sketch of the boundary conditions. The free surface is treated as a rigid lid with free-slip conditions. The bottom is also treated as a free-slip boundary.

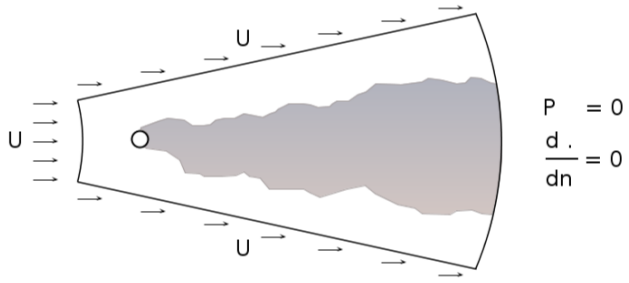

Figure 2: Boundary conditions.

The inflow of the plume consists of a small, vertical downward, pipe with a length of 2 diameters starting at the free surface. The plume inflow needs to be perturbated to evolve from laminar to turbulent. Fluctuations are generated based on plume azimuthal modes. It generates an instable initial flow which quickly transits to turbulent flow. The plume preferred modes determined by a Strouhal number of 0.3 are used. It has been used several times for jet and plume simulations (e.g. Menon and Rizk 1996, Chen et al. 2008, Worthy 2003). The fluctuating component of the velocity at every grid point (i, j) of the plume inflow can be written as:

$$w'(i,j) = \frac{A}{N} W_0 \sum_{n=1}^{N} \sin\left(\frac{2\pi f t}{n} + \theta(i,j)\right), \tag{8}$$

with A as the amplitude of the fluctuations, W_0 is the mean plume inflow velocity, the number of modes $N = 6$, the frequency f chosen such that Strouhal$= \frac{fD}{W_0} = 0.3$, and $\theta(i, j)$ as the azimuthal angle defined from the center of the plume outflow. The amplitude A is set to 0.2, the U, V velocities of the plume are forced with $0.1W_0$. A must be large enough to trigger instabilities, but once large enough the simulation is not very sensitive to the exact value of A. A comparison has been made with A halved and no significant difference was found.

Because the bottom is treated as a free-slip boundary, the cross flow velocity is constant over the vertical. No perturbations are added to the cross flow velocity. So there is no ambient turbulence. The simulations can be regarded as a TSHD sailing in still ambient water. The cross flow velocity in the model is equal to the sailing speed of the TSHD.

VALIDATION DREDGE PLUME IN CROSS FLOW

Plume in cross flow characterisation

A plume in cross flow can be characterised by two independent dimensionless numbers, the plume Richardson number Ri and the velocity ratio ζ:

$$Ri = \frac{g\Delta\rho_0/\rho_a D}{W_0^2}, \tag{9}$$

$$\zeta = \frac{U}{W_0}, \tag{10}$$

where g is the gravitational acceleration, $\Delta\rho_0 = \rho_0 - \rho_a$ is the initial plume density minus the ambient density, D is the initial plume diameter, W_0 is the initial vertical plume velocity and U is the ambient cross flow velocity. The Richardson number Ri is the dimensionless ratio of energy generated by buoyancy compared with the initial kinetic energy of the plume. The higher Ri, the more important buoyancy is. When Ri is very small, buoyancy is negligible. When the velocity ratio ζ is large, the cross flow velocity is larger than the initial vertical velocity of the plume and the initially vertical plume will bend over quickly towards the direction of the ambient flow. When ζ is smaller, bending over of the plume will take longer.

Typical values of a dredge overflow plume are $\Delta\rho_0 = 200$ kg/m^3, $\rho_a = 1030$ kg/m^3, $D_{overflow} = 2$ m, $W_0 = 2$ m/s, U =1.5 m/s. This results in Ri =0.8 and ζ=0.75. But in practice $\Delta\rho_0$, $D_{overflow}$, W_0 and U can vary significantly resulting in a range of $Ri \approx 0.1 - 10$ and $\zeta \approx 0 - 4$ for overflow plumes.

Validation 1

First validation (not shown here) has been carried out by comparing model results of a horizontal plume in cross flow with $Ri = 0.0044$ and $\zeta = 0.2$ against experimental results from Ayoub (1973). These Ri and ζ values are a bit off from a typical overflow plume, but as the plume is ejected horizontally instead of vertically, it is a good test to see the separate influence of the exchange of momentum and density effects. The 3D CFD model captured the experimental results accurately. The location and width of the plume was correct in all three directions.

Validation 2

A more relevant validation has been carried out with a scale experiment of a dredge plume, this validation is discussed here. Eekelen (2007) carried out an experiment of a dredge plume with $\Delta\rho_0 = 50$ kg/m^3, $\rho_a = 1000$ kg/m^3, $D = 0.01$ m, $W_0 = 0.05$ m/s and $U = 0.04$ m/s for his Masters thesis. Due to the facilities available he could not use larger dimensions, but in his experiment a plume is generated with $Ri = 2$, and $\zeta = 0.8$. These values are close to the typical dredge plume values of Ri =0.8 and ζ=0.75. Only remaining scaling issue is the Reynolds number of the experiment. $Re = \frac{W_0 D}{\nu} = 500$ does not exceed 2000-4000, what is needed to reach a fully developed state (Fischer et al. 1979).

The experiment of Eekelen (2007) has been simulated with the 3D CFD model. Figure 3 shows an instantaneous plot of contours of the plume concentrations. As can be seen the whirls and irregularities well known for plumes are also visible in the model results. When going down, the plume entrains cross flowing water. The plume expands, dilutes and bents over with the cross current. In the experiment, plume concentrations are measured at three cross sections, 25D, 40D and 54D downstream. A comparison between the time averaged modelled concentrations and the measured ones is depicted in Figure 4. The shape and dilution of the modelled plume compares good with the measurements. The characteristic kidney shaped profile develops correctly in the model. At 54D downstream both the model and experiment show a start of plume divergence. The vertical position of the plume is higher in the model results than in the measurements. This can be caused by some differences between the experiment and the model input. First of all a

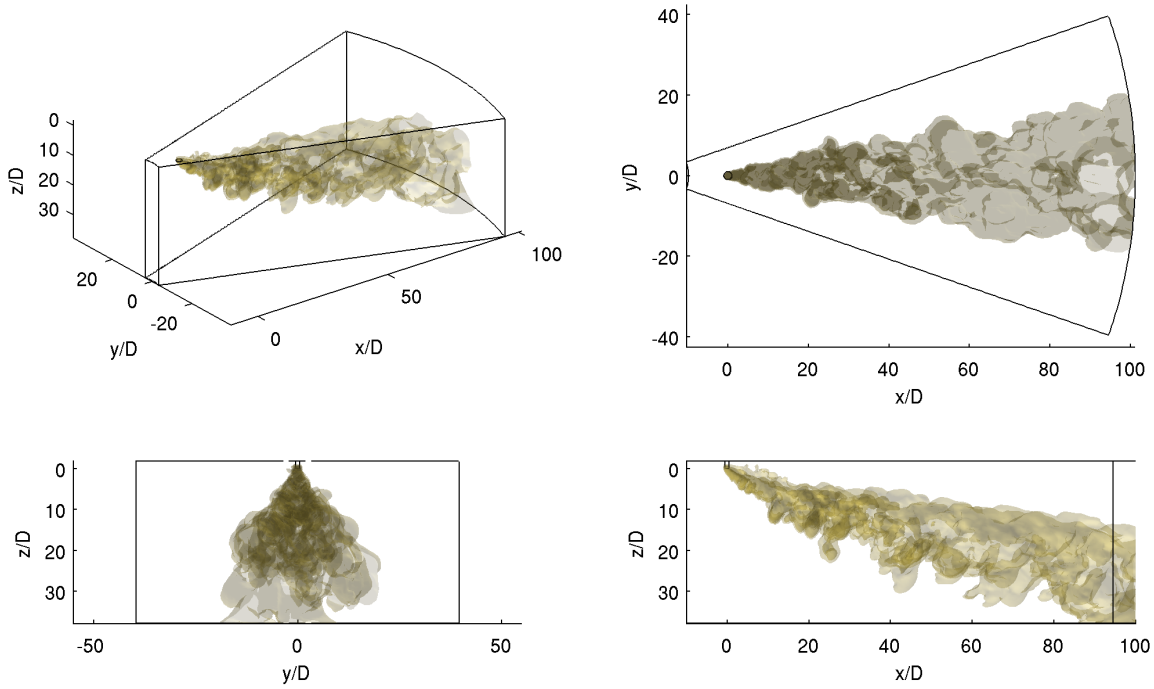

Figure 3: 3D CFD model result dredge plume.

scaled vessel has been used around the outflow tube in the experiments to mimic a TSHD. In the CFD model simply a vertical outflow is used without vessel. Another difference is that in the experiment the cross flow is turbulent and has a log-shape towards the bed as in the CFD model the cross flow is constant over depth and without fluctuations. Last important difference is about the sediment input flux. In the model this is constant in time, where in the experiment this turned out to be impossible. During each experimental run the input flux shifted an unknown arbitrary bit. Given these differences between the experiment and the CFD model, the model results are satisfactory.

TRANSITION FROM DENSITY DRIVEN TO MIXING BEHAVIOUR OF AN OVERFLOW PLUME

Explanation simulations

To show some of the capabilities of the CFD model, the transition of an overflow plume from density driven to mixing behaviour is investigated. Given enough distance, every plume in cross flow will eventually undergo this transition. Density differences are then no longer the important driving force. A plume with high Ri in a weak cross flow (ζ low) will remain density driven for a long distance. And a plume with low Ri and high ζ will need a short distance to become dominated by the ambient currents. Winterwerp (2002) has investigated the transition from density driven to mixing behaviour for overflow plumes for several combinations of Ri and ζ. In that study the transition was investigated at a fixed depth, at the bed in the experimental flume. The water depth was 8 times the initial diameter of the overflow. Therefore the diagram in that study is a transition diagram for a depth of 8D. When another depth is considered, another diagram is needed. In this study a diagram will be constructed which is valid for many depths. In contrast with the experiments not only limited point measurements and photos/videos are available, but 3D data about concentrations, densities and velocities can be extracted from the CFD model. So instead of focusing on the question whether the plume is still density driven at the bed, now more general, the transition location in the water column is investigated. Several CFD calculations will be used to find the vertical distance a plume has to travel where

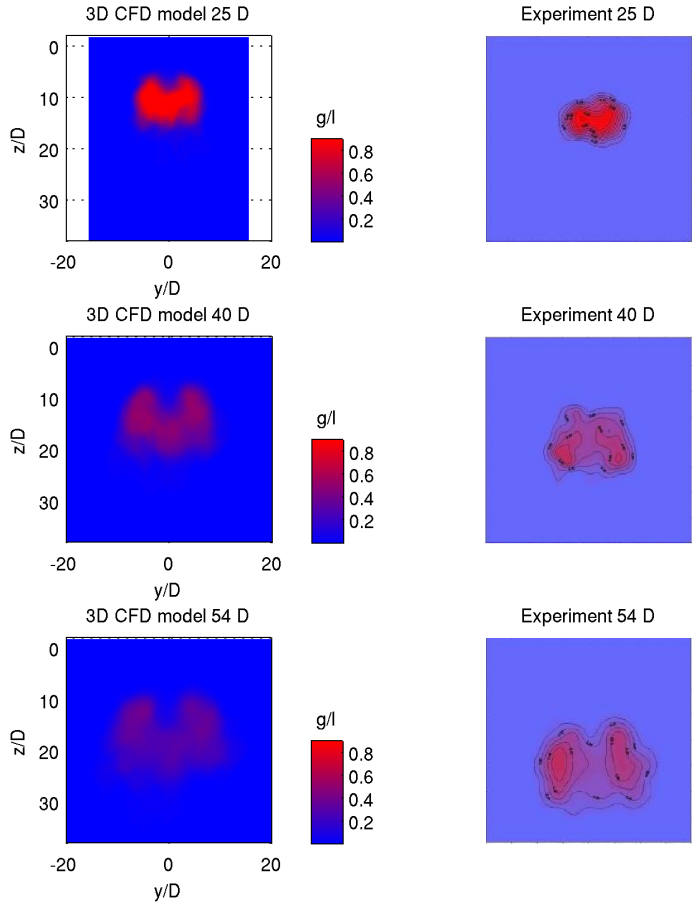

Figure 4: Comparison plume concentration 3D CFD model and experiment ($Ri = 2, \zeta = 0.8$).

the density differences are no longer the dominant driving force. In Figure 5 the classification found by Winterwerp (2002) is shown, together with the CFD calculations carried out in this study. The Eekelen (2007) validation run ($Ri = 2$,$\zeta = 0.8$) is used as base run. Around this run a whole series of CFD runs is defined which envelop the whole Ri,ζ range which has relevance for overflow plumes.

Transition criterium

In order to find the depth where a plume becomes cross flow driven instead of density driven, a transition criterium is needed. Winterwerp (2002) used the front speed of the radially spreading sediment layer on the bed to assess whether it is still density driven or not. This criterium is insufficient now, a more general criterium is needed which is applicable all over the water column. The transition from density driven behaviour towards cross flow driven behaviour means that the buoyancy was important but after the transition it can be neglected. The importance of buoyancy compared with kinetic energy is given by the Richardson number. Therefore a locally determined Richardson number is a suitable candidate as transition parameter. In this study a local plume Richardson number $Ri_l < 0.15$ is used, it is defined by:

$$Ri_l = \frac{g\Delta\rho_l/\rho_a D_l}{U^2} < 0.15, \tag{11}$$

with $\Delta\rho_l = \rho_l - \rho_a$, ρ_l is given by the local centerline density of the plume, and D_l is the local plume width defined by a top hat profile. The edge of a top hat profile coincides with the visual edge of a plume and the 50% velocity

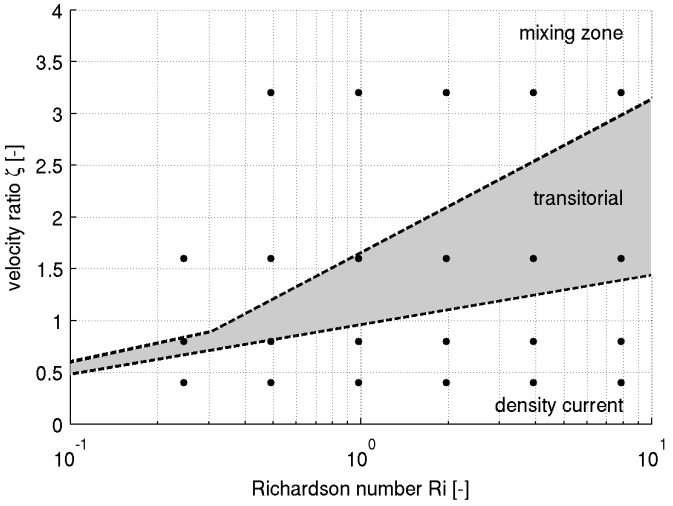

Figure 5: CFD calculations shown as dots in Ri,ζ diagram with the classification found by Winterwerp (2002) shown as lines.

intermittency location (Lee and Chu 2003). The time averaged CFD results are used to obtain the plume path on the (x, z) center face. The local centerline density ρ_l follows directly from the CFD results. D_l is calculated using conservation of plume volume:

$$C_l \frac{\pi}{4} D_l^2 U_l = C_0 \frac{\pi}{4} D^2 W_0, \tag{12}$$

where C_l and U_l are the center line plume concentration and velocity found from time averaged CFD results. The initial plume values C_0, D, W_0 are known, therefore Equation 12 gives D_l. Using this approach, D_l can be found everywhere along the centerline of the bended plume in cross flow in a quick and robust way. D_l for x =25D, 40D, 54D in Figure 4 is 9.3D, 14.2D and 18.6D respectively. Which agrees with a visual estimate of D_l. An example of the time averaged CFD center face results can be seen in Figure 6. The location where $Ri_l < 0.15$ the centerline marks switch from green '.' towards blue 'o'.

The transition of density driven plume behaviour towards mixing behaviour is defined at $Ri_l < 0.15$. The transition found in this way is in line with the transition found by Winterwerp (2002). A value of 0.15 is also in line with Turner (1973) who found critical values of 0.1-0.2 for density currents at a bed. To assess grid independence a calculation with a finer grid (3x more cells) has been carried out. Both simulations differed less then 5% in transition depth. Another validation has been undertaken with three simulations where the initial $\Delta\rho$, D, W, U are doubled and halved in such way that Ri and ζ remained the same. The highest transition depth was 10% larger than the smallest one. In these runs Re was not constant, but the results are very close to each other. So although Re did not exceed 2000-4000 which is necessary for truly turbulent flow, it is not an important issue. These two validations give confidence in the developed procedure to find the transition depth.

Transition depths overflow plumes

For each CFD calculation shown in the Ri,ζ diagram of Figure 5 a transition depth is determined from the simulation results. These transition depths are interpolated to iso-contours as shown in Figure 7. The influence of the depth on the behaviour of a plume is now made visible. On the horizontal axis, the Ri number indicates the importance of buoyancy of a plume. Moving to the right the Ri number of a plume increases and buoyancy gets more important

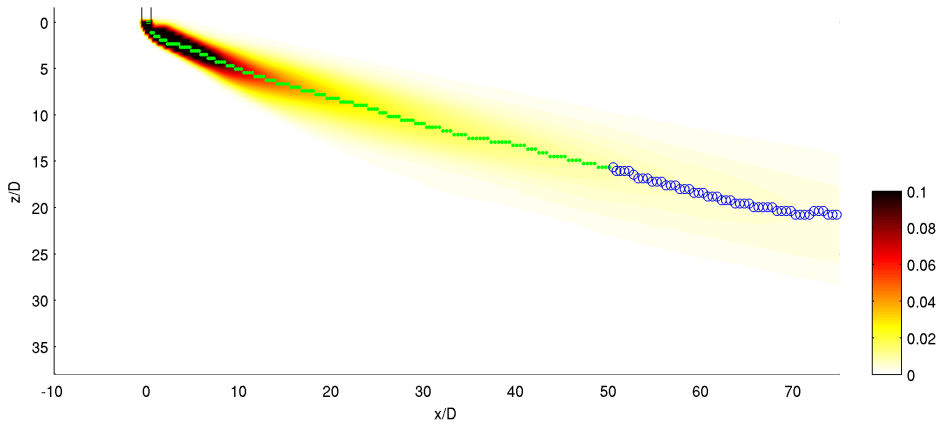

Figure 6: Example of time averaged CFD dredge plume results on the center face ($Ri = 1, \zeta = 0.8$). C is shown as colored surface and the plume centerline marker is shown as green '.' if $Ri_l > 0.15$ and as blue 'o' if $Ri_l < 0.15$. The transition depth in this figure is 16D.

(the plume gets heavier). Moving to the right also the transition depth increases, this means that a heavier plume needs a longer transition depth where buoyancy no longer is important. Moving up in the figure means the velocity ratio ζ increases and the ambient velocity becomes more important. A plume with a higher velocity ratio ζ has a smaller transition depth, it needs a shorter distance to become mixing dominated. An overflow plume which stays density driven up to the seabed in one depth, can shift to mixing behaviour at a deeper seabed. In the Ri, ζ diagram the transition contours are convex curves. Because the contours are interpolated in between only limited points, they should be used to indicate the trend rather than the exact transition depth up to decimal accuracy.

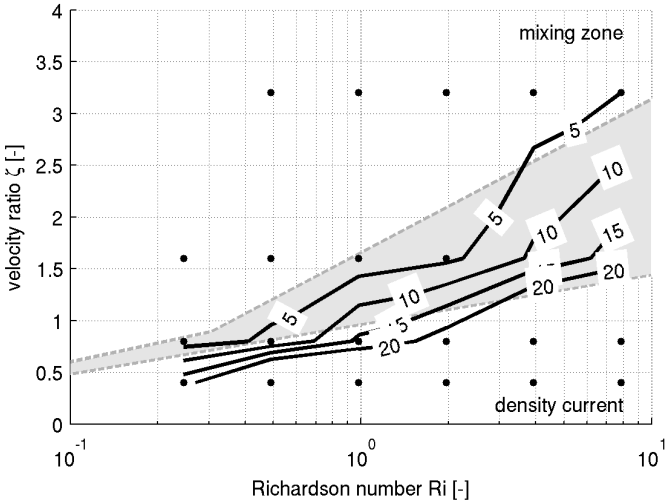

Figure 7: Transition depth contours (5D, 10D, 15D, 20D) obtained from CFD calculations shown as solid lines. When for example dredging is carried out in a depth of 10D and the dredge plume (Ri, ζ) is above the 10D line in this diagram, it will have made the transition towards mixing behaviour before the seabed is reached. When (Ri, ζ) is under the 10D line, it is expected to be density driven all the way to the seabed. The transition results of Winterwerp (2002) are shown as dashed grey lines (obtained for depth = 8D).

Winterwerp (2002) investigated the transition at a fixed depth of 8 diameters. So that result can be regarded as a

8D transition depth contour. In fact it is not presented as a sharp contour, but a transitional zone in between density driven behaviour and mixing behaviour is defined. The 8D contour (in between the 5D and 10D contours shown in Figure 7) from this study follows the lower boundary of Winterwerp (2002) at low Ri numbers and moves through the transition zone up to the upper boundary of Winterwerp (2002) at high Ri numbers. There are some differences between the experimental data Winterwerp (2002) used and the CFD model data used in this study. In the experiment the plume outflow was fixed and the cross current was generated in a flume. So in the experiment there was a log velocity profile and ambient turbulence, in the CFD model the cross current is constant over the vertical and there is no ambient turbulence. And both studies have used different criteria to determine whether the flow is density driven. Despite these differences the results are comparable.

CONCLUSIONS AND RECOMMENDATIONS

A dedicated 3D CFD model for dredge plumes has been presented. It is non hydrostatic and density differences are fully taken into account. State of the art LES technique is used to capture turbulent fluctuations. The grid, schematisation and boundary conditions are optimised for dredge plume problems. At this moment the CFD model can simulate general (dredge) plumes in cross flow. The CFD model results have been validated against plume in cross flow experimental data. Shape and dilution of the plume are accurately reproduced in the model.

The CFD model has been used to find the transition depth where a dredge plume becomes cross flow dominated in stead of density driven. With Ri_l in Equation 11 a suitable transition criterium is defined. Several calculations have been carried out, spanning the total Ri,ζ range of possible dredge plumes. Figure 7 shows that a dredge plume with high Ri and low ζ stays density driven up to a large depth. A dredge plume with low Ri and high ζ on the other hand needs only a small depth to become mixing dominated. The results are in line with the results of Winterwerp (2002).

Future planned extensions of the model will include processes important for overflow plumes, like air entrainment, interaction with the vessel, interaction with the sea bed and incorporation of different sand/mud fractions. More experimental validation data is needed with Ri,ζ numbers relevant for dredge plumes. The scale of these experiments needs to be such that Re remains >2000-4000. In the end also validation with real scale dredge plume measurements around TSHDs is necessary. Some field measurement campaigns have been carried out already and some more are being planned.

REFERENCES

Ayoub, G. M. (1973). Test results on buoyant jets injected horizontally in a cross flowing stream. *Water, Air and Soil Pollution 2*, 409–426.

Chen, Y., C. Li, and C. Zhang (2008). Numerical modeling of a round jet discharged in random waves. *Ocean Engineering 35*, 77–89.

Eekelen, E. (2007). Experimental research on dynamic dredge overflow plumes. Master's thesis, TU Delft. Civil Engineering.

Fischer, H., J. Imberger, E. List, R. Koh, and N. Brooks (1979). *Mixing in inland and coastal waters*. Academic Press.

Hirsch, C. (1990). *Numerical computation of internal and external flows*. A Wiley Interscience Publication.

Lee, J. and V. Chu (2003). *Turbulent jets and plumes*. Kluwer Academic Publishers.

Menon, S. and M. Rizk (1996). Large-eddy simulations of forced three dimensional impinging jets. *International Journal of Computational Fluid Dynamics 7*, 275–289.

Nakata, K., Y. Okayama, and J. Lavelle (1989). An attempt to evaluate the effects of an anti-turbidity system on sediment dispersion from a hopper dredge. *NOAA Technical Memorandum ERL PMEL-85 0*, 1–30.

Nichols, M., R. Diaz, and L. Schaffner (1990). Effects of hopper dredging and sediment dispersion, chesapeake bay. *Environmental Geology and Water Sciences 15*(1), 31–43.

Pourquié (1994). *Large Eddy Simulation of a turbulent jet*. Ph. D. thesis, Delft University of Technology.

Turner, J. (1973). *Buoyancy effects in fluids*. Cambridge University Press.

Whiteside, P., K. Ooms, and G. Postma (1995). Generation and decay of sediment plumes from sand dredging overflow. *Proceedings of the 14th world dredging congress 2*, 877–892.

Winterwerp, J. (2002). Near-field behavior of dredging spill in shallow water. *Journal of waterway, port, coastal and ocean engineering 128*(2), 96–98.

Worthy, J. (2003). *Large Eddy Simulation of buoyant plumes*. Ph. D. thesis, Cranfield University.

ACKNOWLEDGMENTS

This PhD study is carried out as part of the Building with Nature research program. The financial support and interaction with other research carried out within Building with Nature is highly appreciated. A.M. Talmon is acknowledged for his feedback.

NOMENCLATURE

Symbol	Units	Definition
A	-	Amplitude azimuthal forcing plume inflow
C	-	Plume volume concentration
C_0	-	Initial plume volume concentration
C_l	-	Local centerline plume volume concentration
Cs	-	Smagorinsky constant (0.1)
D	m	Initial plume diameter (equal to overflow diameter)
D_l	m	Local centerline plume diameter
f	1/s	Frequency used in azimuthal forcing plume inflow
$\boldsymbol{f}$	m/s^2	Body force acceleration vector (gravity)
g	m/s^2	Gravitational acceleration
L_f	-	Filter width sub-grid-scale model
P	Pa	Pressure
Re	-	Reynolds number
Ri	-	Plume Richardson number
Ri_l	-	Local plume Richardson number
$\boldsymbol{S}$	1/s	Rate of strain tensor
Sc	-	Schmidt mixing coefficient
t	s	Time
U	m/s	Horizontal cross flow velocity
$\boldsymbol{u}$	m/s	Velocity vector
W_0	m/s	Plume inflow velocity
Γ	m^2/s	Diffusion coefficient
ζ	-	Velocity ratio
θ	m/s	Azimuthal angle defined from center of plume outflow
ν	m^2/s	Kinematic viscosity
ν_{mol}	m^2/s	Kinematic molecular viscosity
ν_{sgs}	m^2/s	Sub grid scale kinematic viscosity
ρ	kg/m^3	Mixture density
ρ_0	kg/m^3	Initial plume density
ρ_a	kg/m^3	Ambient density
ρ_l	kg/m^3	Local centerline plume density
$\boldsymbol{\tau}$	N/m^2	Shear stress tensor